arXiv:nucl-th/0103059v1 23 Mar 2001

VECTOR MESON DECAY OF BARYON RESONANCES

U. MOSEL AND M. POST*
Institut für Theoretische Physik, Universität Giessen, D-35392 Giessen
**Email: Marcus.Post@theo.physik.uni-giessen.de*

We investigate the coupling of vector mesons with nucleons to nucleon resonances in an isospin-selective VMD approach and explore the in-medium properties of vector mesons.

1 Introduction

One of the evidences for the discovery of a new state of matter that was quoted by the CERN press release in 2000 was the result of the CERES experiment[1] that showed an excess of dileptons at invariant masses below the vector meson mass. In order to understand this phenomenon it is essential to consider the effect of conventional hadronic interactions on the vector mesons. We emphasize the relevance of the excitation of baryon resonances in this context. To this end we analyze the decay of nucleon resonances into vector mesons within an isospin selective VMD model. In the isovector channel we compare the results to fits to the hadronic $N\rho$ decay width. In the isoscalar channel we then predict the ω coupling strength.

2 VMD Analysis of the Electromagnetic Resonance Decay

Vector Meson Dominance (VMD)[2], a theory which describes photon-hadron interactions exclusively in terms of vector meson-hadron interactions, relates the hadronic coupling strength of resonances to vector mesons $f_{RN\rho(\omega)}$ and the isoscalar and isovector part of the photon-coupling:

$$f_{RN\omega} = g_s\, m_\omega\, \frac{2\, g_\omega}{e} \quad , \quad f_{RN\rho} = g_v\, m_\rho\, \frac{2\, g_\rho}{e} \quad . \tag{1}$$

As values for g_ρ and g_ω – the coupling strengths of ρ and ω meson to the photon – we take $g_\rho = 2.5$ and $g_\omega = 8.7$ (ref. [2]). The isoscalar and isovector coupling strength of the resonance to the $N\gamma$ system is given by g_s and g_v, respectively, see Eq. 2. Thus VMD gives access to both $f_{RN\omega}$ and $f_{RN\rho}$, if it is possible to obtain g_s and g_v from experimental data. In order to achieve this goal, the coupling has to be decomposed into an isoscalar and an isovector part, which is readily done by constructing suitable linear combinations of proton- and neutron-amplitudes[3].

The isospin part I of the electromagnetic coupling is given by:

$$I = \chi_R^{I\,\dagger}\ (g_s + g_v\,\tau_3)\ \chi_N^I \tag{2}$$

For simplicity we restrict ourselves here to the case of isospin 1/2; the case of isospin 3/2 contains additional Clebsch-Gordan coefficients which are given in ref.[3]. The spinors χ_R^I and χ_N^I represent resonance and nucleon iso spinors and I_R denotes the isospin of the resonance. τ_3 refers to the Pauli matrix. From the structure of the isospin coupling I it follows that the linear combinations

$$\mathcal{M}_{s/v} = \frac{1}{2}\ (\mathcal{M}_p \pm \mathcal{M}_n) \tag{3}$$

are proportional to g_s and g_v respectively.

At the pole-mass of the resonance the helicity amplitudes $A^{p/n}_{\frac{1}{2}}$ and $A^{p/n}_{\frac{3}{2}}$ are known from experiment. Therefore also g_s and g_v are determined except for a normalization factor. We calculate this factor by introducing the γ-width $\Gamma^{\gamma}_{s/v}$, defined in terms of the helicity amplitudes $A_{s/v}$ as follows[4]:

$$\Gamma^{\gamma}_{s/v}(m_R) = \frac{\mathbf{q_{cm}}^2}{\pi}\,\frac{2m_N}{(2j_R+1)m_R}\,\left(|A^{s/v}_{\frac{1}{2}}|^2 + |A^{s/v}_{\frac{3}{2}}|^2\right) \quad , \tag{4}$$

with j_R and m_R denoting spin and pole-mass of the resonance and $\mathbf{q_{cm}}$ the cm-momentum of the photon. Clearly, $\Gamma^{\gamma}_{s/v}$ can also be expressed using Feynman amplitudes:

$$\Gamma^{\gamma}_{s/v}(k^2) = \frac{1}{(2j_R+1)}\,\frac{\mathbf{q_{cm}}}{8\,\pi\,k^2}\,|\mathcal{M}_{s/v}|^2 \quad , \tag{5}$$

where $\sqrt{k^2}$ is the invariant mass of the resonance. After summing over the photon polarizations, $|\mathcal{M}_{s/v}|^2$ assumes the following form:

$$|\mathcal{M}_{s/v}|^2 = 4\,m_N\,m_R\,\kappa\,g^2_{s/v}\,q^2\,F(k^2) \quad . \tag{6}$$

The formfactor $F(k^2)$ at the $RN\gamma$ vertex is taken from ref.[5]. The numerical factor κ depends on the quantum numbers of the resonance (ref.[3]). The two expressions Eqs. 4 and 5 can now be equated allowing to solve for $g_{s/v}$:

$$g^2_{s/v} = \frac{4}{\kappa}\,\frac{|A^{s/v}_{\frac{1}{2}}|^2 + |A^{s/v}_{\frac{3}{2}}|^2}{\mathbf{q_{cm}}} \tag{7}$$

In this way it is possible to obtain $g_{s/v}$ from helicity amplitudes. The hadronic couplings $f_{RN\omega(\rho)}$ are then readily deduced from the VMD relation Eq. 1. The corresponding values are listed in Tables 1 and 2.

3 The ρ Meson

3.1 VMD in the Isovector Channel

In this section we investigate the applicability of VMD for the isovector channel of the resonance decay. For the helicity amplitudes we use different parameter sets in order to provide an estimate for the experimental uncertainties entering this analysis. They are taken from Arndt *et al*[6] and Feuster *et al*[5]. The ρ decay widths are taken from the analysis of Manley *et al*[7].

In Table 1 the results for the coupling constants and the corresponding error-bars are given. As a general tendency, VMD works well within a factor of two. This can be seen particularly well in the case of the $D_{13}(1520)$ and the $F_{15}(1680)$, which are the most prominent resonances in photon-nucleon reactions, and whose ρ decay widths are also well under control. Note in particular the large coupling constant for the $D_{13}(1520)$ in the hadronic fit which is possible only because of the large width of the ρ meson[8,9].

For the $P_{13}(1720)$ and the $F_{35}(1905)$ resonances VMD is off by an order of magnitude. We argue that this mismatch does not necessarily indicate a failure of VMD, but can be traced back to the unsatisfactory experimental information on these two resonances. Neither the helicity amplitudes nor the partial $N\rho$ width are well determined from experiment[5,6,7]. Obviously, the extraction of the resonance parameters is very complicated and might be sensitive to the details of the underlying theoretical model, such as the treatment of the non-resonant background. For a conclusive VMD analysis of these resonances it is therefore mandatory to enlarge the data base and to describe hadron- and photoinduced reactions within one and the same

	$f_{RN\rho}$(Arndt)	$f_{RN\rho}$(Feuster)	$f_{RN\rho}$(Manley)
$D_{13}(1520)$	3.44±0.18	2.67	6.67±0.78
$S_{31}(1620)$	0.89±0.42	0.10	2.14±0.30
$S_{11}(1650)$	0.70±0.08	0.59	0.47±0.19
$F_{15}(1680)$	3.48±0.39	—	6.87±1.57
$D_{33}(1700)$	3.96±0.77	3.68	1.962±0.67
$P_{13}(1720)$	0.25±0.42	0.93	13.17±3.35
$F_{35}(1905)$	2.47±0.55	—	17.97±1.14
$P_{33}(1232)$	13.40±0.2	11.96	—

Table 1. Results for $f_{RN\rho}$ from a VMD analysis (1st and 2nd column) and a hadronic fit (3rd column).

analysis.

We conclude that VMD works remarkably well in the isovector channel. Therefore, our approach should yield reasonable predictions of the unknown coupling constants $f_{RN\omega}$.

3.2 The ρ Spectral Function in Nuclear Matter

Using the coupling constants obtained from the hadronic $N\rho$ decay width of the resonance, we calculate the spectral function $A_\rho^{T/L}(\omega, \mathbf{q})$ of the ρ meson in nuclear matter[8,9] at density $\rho = \rho_0$. It is defined as:

$$A_\rho^{T/L}(\omega, \mathbf{q}) = \frac{1}{\pi} \frac{\text{Im } \Sigma^{T/L}(\omega, \mathbf{q})}{(\omega^2 - \mathbf{q}^2 - m_\rho^2 + \text{Re } \Sigma^{T/L}(\omega, \mathbf{q}))^2 + \text{Im } \Sigma^{T/L}(\omega, \mathbf{q})^2} \quad . \tag{8}$$

Note that in nuclear matter transverse and longitudinal modes – denoted by T and L, respectively – have to be treated independently. Here ω and $\mathbf{q}$ denote energy and momentum relative to the rest frame of nuclear matter. The selfenergy $\Sigma^{T/L}(\omega, \mathbf{q})$ is a sum of vacuum and in-medium contributions. The vacuum part is given by the 2-pion decay mode and we estimate the in-medium part within the low-density approximation:

$$\Sigma_{med}^{T/L}(\omega, \mathbf{q}) = \frac{1}{8m_N} \rho_N T_{tot}^{T/L}(\omega, \mathbf{q}) \quad . \tag{9}$$

The main quantity entering this expression is the ρN forward scattering amplitude $T_{tot}^{T/L}$. In Fig. 1 we show the results for $A_\rho^{T/L}(\omega, \mathbf{q})$. They highlight an important consequence of the strong coupling of the $D_{13}(1520)$ to the $N\rho$ system, namely the strong modification of the ρ spectral function in nuclear matter. In particular at low momenta the mass spectrum is dominated by the excitation of a $D_{13}(1520)$, leading to a substantial shift of spectral strength down to lower invariant masses. This, of course, is of relevance for the interpretation of the CERES data. At large momenta the $P_{13}(1720)$ and the $F_{35}(1905)$ dominate the spectrum. The predominant feature is the different modification of transverse and longitudinal ρ mesons.

4 The ω Meson

4.1 VMD in the Isoscalar Channel

In this section we present our results for the coupling constants $f_{RN\omega}$ and discuss their compatibility with experimental information obtained from pion- and photon-induced ω-production cross sections.

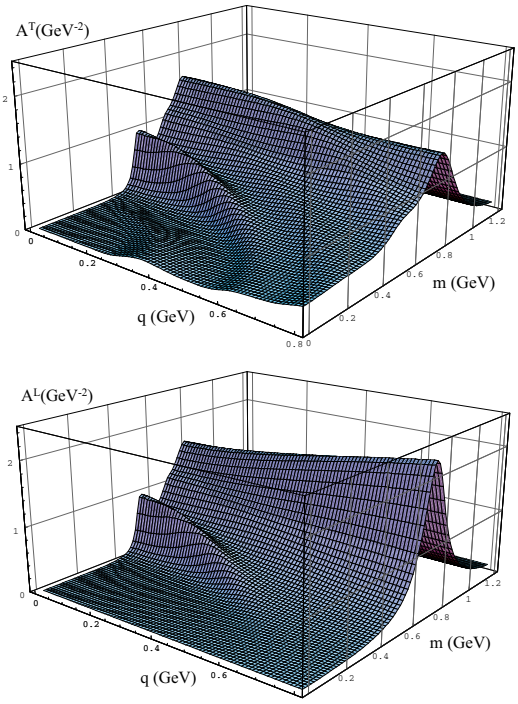

Figure 1. Top: A_ρ^T as a function of invariant mass m and 3-momentum $\mathbf{q}$. Bottom: Same for A_ρ^L.

All nucleon resonances with $j_R < \frac{7}{2}$, for which helicity amplitudes have been extracted, are included. Thus we consider only one resonance above the $N\omega$ threshold in our analysis, namely the $D_{13}(2080)$. We use again the helicity amplitudes from Arndt *et al*[6] and Feuster *et al*[5]and consider also the PDG estimates[4]. The corresponding results for $f_{RN\omega}$ together with the errorbars are given in Table 2. We find a strong coupling to the $N\,\omega$ channel in the S_{11}, D_{13} and F_{15} partial waves; especially the $S_{11}(1650)$, the $D_{13}(1520)$ and the $F_{15}(1680)$ resonances show a sizeable coupling strength to this channel.

It is noteworthy that the resonances with the largest coupling are well below the $N\omega$ threshold. Subthreshold resonances in the $N\omega$ channel are also reported elsewhere[10,11]. The coupled-channel analysis[10] of $\pi\,N$ scattering enforces resonant structures in the $N\omega$ channel, in particular in the S_{11} and D_{13} partial waves. However, the coupling strength extracted in their analysis is

	$f_{RN\omega}$(Arndt)	$f_{RN\omega}$(Feuster)	$f_{RN\omega}$(PDG)
$S_{11}(1535)$	1.27±1.58	1.36	0.76±1.23
$S_{11}(1650)$	1.59±0.29	0.56	1.12±1.09
$D_{13}(1520)$	2.87±0.76	2.28	3.42±0.87
$D_{13}(1700)$	− − −	1.88	0.65±2.76
$D_{13}(2080)$	− − −	− − −	1.13±1.46
$P_{11}(1440)$	0.61±0.68	1.26	0.85±0.48
$P_{11}(1710)$	0.14±0.85	0	0.20±1.02
$P_{13}(1720)$	0.29±1.30	2.18	1.79±3.18
$F_{15}(1680)$	6.89±1.38	− − −−	6.52±1.49

Table 2. VMD predictions for the coupling strength $f_{RN\omega}$.

$f_{RN\omega} \approx 6.5$, nearly twice as large as our value. In the quark model calculation of ref.[11] a value of about $f_{RN\omega} \approx 2.6$ is found, which is surprisingly close to our result.

The quality of the VMD predictions can further be tested by a comparison with experimental data on the reactions $\pi^- p \to \omega n$ and $\gamma p \to \omega p$. Comparison with data allows also to discuss the results for the $D_{13}(2080)$, the only resonance in our analysis above threshold. We find for this resonance an ω decay width of about 70 MeV and argue that its contribution to both reactions is too small to be seen in experiment. As a first approximation, we take the full production amplitude as an incoherent sum of *Breit-Wigner* type amplitudes, describing s-channel contributions.

The results are shown in Fig. 2. The data for the π-induced reaction are taken from ref.[12] and we use the photoproduction data of ref.[13]. The cross-section for $\pi^- p \to \omega n$ is reproduced rather well near threshold. This is in agreement with the findings of ref.[10], where a satisfactory description of this process around threshold in terms of near or subthreshold resonances is presented. This suggests that the excitation of subthreshold resonances constitutes an essential ingredient to the production mechanism. The contribution coming from the only resonance above threshold – the $D_{13}(2080)$ – is about 0.1 mb, roughly 10% of the total cross-section.

On the other hand, the photoproduction data cannot be saturated within the resonance model; this gives little hope to find the $D_{13}(2080)$ in this reaction. However, adding the contribution from π^0-exchange yields a qualitative explanation of the data over the energy range under consideration.

Overall it seems that the predictions of the resonance model are in reasonable agreement with the data and can be viewed as a confirmation of the

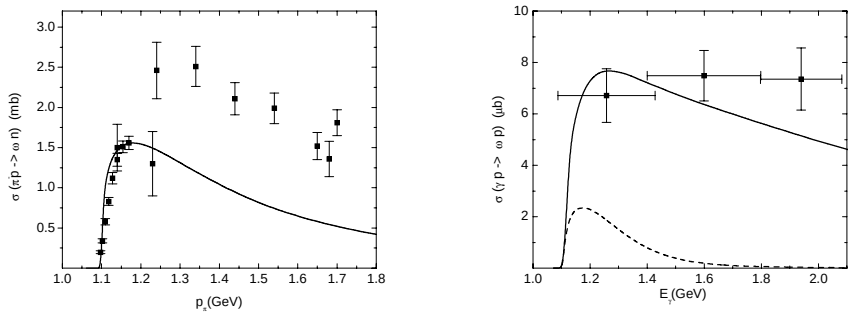

Figure 2. Left: Total cross-section for the reaction $\pi^- p \to \omega n$. Right: Total cross-section for the reaction $\gamma p \to \omega p$ with resonance contribution only (dashed line) and added pion-exchange (solid line).

VMD analysis.

4.2 The ω Spectral Function in Nuclear Matter

Within the same formalism as for the ρ meson we investigate the effects of resonance-excitation on the properties of ω mesons in nuclear matter. Again the calculations are performed at $\rho = \rho_0$. We find a broadening of the ω meson of about 50 MeV and a repulsive mass shift of roughly 20 MeV, see Fig. 3. These findings are in surprising agreement with those of various other groups[10,14,15]. The ω meson thus is much less modified in nuclear matter than the ρ meson, which follows within our model from the much smaller coupling constants. As can be seen in Fig. 3 the in-medium effects are most pronounced at small momenta.

5 Conclusions

We have demonstrated that through the excitation of baryon resonances the in-medium spectral functions of vector mesons receive a substantial shift of spectral strength down to lower invariant masses. These effects play a key role in understanding the in-medium properties of vector mesons.

6 Acknowledgments

This work was supported by DFG and BMBF.

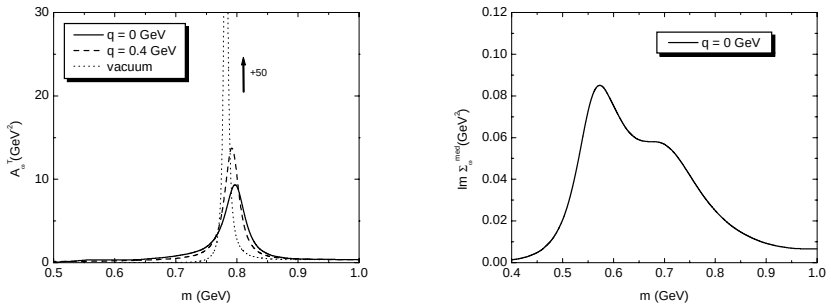

Figure 3. Left: $A_\omega^{T/L}$ at momenta 0 GeV (straight) and 0.4 GeV (dashed). For comparison also the vacuum result is shown (dotted). Right: The imaginary part of the ω selfenergy.

References

1. G. Agakichiev et al., CERES collaboration, *Phys. Rev. Lett.* **75**, 1272 (1995).
2. H. B. O'Connell, B. C. Pearce, A. W. Thomas and A. G. Williams, *Prog. Part. Nucl. Phys.* **39**, 201 (1997).
3. M. Post and U. Mosel, *Nucl. Phys.* A (2001) in press, e-print Archive: nucl-th/0008040.
4. Particle Data Group, *Eur. Phys. J.* C **3**, 1 (1998).
5. T. Feuster and U. Mosel, *Phys. Rev.* C **59**, 460 (1999).
6. R. A. Arndt *et al.*, *Phys. Rev.* C **52**, 2120 (1995).
7. D.M. Manley and E.M. Saleski, *Phys. Rev.* D **45**, 4002 (1992); *Phys. Rev.* D **30**, 904 (1984).
8. W. Peters, M. Post, H. Lenske, S. Leupold and U. Mosel, *Nucl. Phys.* A **45**, 4002 (1992).
9. M. Post, S. Leupold and U. Mosel, *Nucl. Phys.* A (2001) in press, e-print Archive: nucl-th/0008027.
10. B. Friman, M. Lutz and G. Wolf, e-Print Archive: nucl-th/0003012.
11. D. O. Riska and G. E. Brown, *Nucl. Phys.* A **679**, 577 (2001).
12. A. Baldini *et al.*, Landolt-Börnstein, vol 1/12 a (Springer, Berlin, 1987).
13. ABBHHM-Colloboration, *Phys. Rev.* **75**, 1669 (1968).
14. F. Klingl, N. Kaiser and W. Weise, *Nucl. Phys.* A **624**, 527 (1997).
15. M. Effenberger, E.L. Bratkovskaya, W. Cassing and U. Mosel, *Phys. Rev.* C **60**, 27601 (1999).